ACS chemical biology

Articles

pubs.acs.org/acschemicalbiology

A Unique Small Molecule Inhibitor of Enolase Clarifies Its Role in Fundamental Biological Processes

Da-Woon Jung,[†,∥] Woong-Hee Kim,[†,∥] Si-Hwan Park,[†] Jinho Lee,[†] Jinmi Kim,[†] Dongdong Su,[#] Hyung-Ho Ha,[‡] Young-Tae Chang,[#,§] and Darren R. Williams*[,†]

[†]New Drug Targets Laboratory, School of Life Sciences, Gwangju Institute of Science and Technology, 1 Oryong-Dong, Buk-Gu, Gwangju 500-712, Republic of Korea

[‡]College of Pharmacy, Sunchon National University, Sunchon, 570-742, Korea

[#]Department of Chemistry, National University of Singapore and MedChem Program of Life Sciences Institute, National University of Singapore, 3 Science Drive 3, Singapore 117543

[§]Laboratory of Bioimaging Probe Development, Singapore Bioimaging Consortium, Agency for Science, Technology and Research (A*STAR), Singapore 138667

Supporting Information

ABSTRACT: Enolase is a component of the glycolysis pathway and a "moonlighting" protein, with important roles in diverse cellular processes that are not related to its function in glycolysis. However, small molecule tools to probe enolase function have been restricted to crystallography or enzymology. In this study, we report the discovery of the small molecule "ENOblock", which is the first, nonsubstrate analogue that directly binds to enolase and inhibits its activity. ENOblock was isolated by small molecule screening in a cancer cell assay to detect cytotoxic agents that function in hypoxic conditions, which has previously been shown to induce drug resistance. Further analysis revealed that ENOblock can inhibit cancer cell metastasis *in vivo*. Moreover, an unexpected role for enolase in glucose homeostasis was revealed by *in vivo* analysis. Thus, ENOblock is the first reported enolase inhibitor that is suitable for biological assays. This new chemical tool may also be suitable for further study as a cancer and diabetes drug candidate.

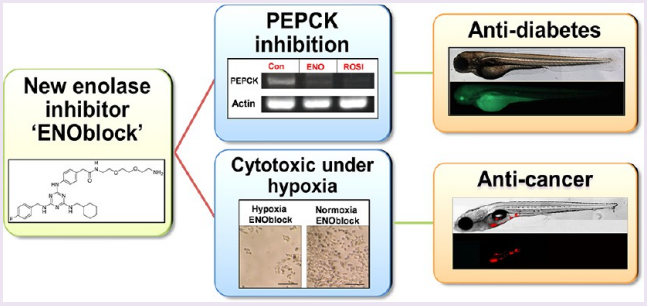

Glycolysis is an ancient and highly conserved metabolic pathway that converts 1 mol of glucose into 2 mol of pyruvate. Free energy is released and used to form the high-energy-containing compounds adenosine triphosphate (ATP) and reduced nicotinamide adenine dinucleotide (NADH). Glycolysis comprises 10 biochemical reactions, and each step is catalyzed and regulated by a different enzyme. Over the past 20 years, there has been increasing appreciation of the multiple roles glycolytic enzymes play in diverse cellular processes (reviewed in ref 1).

Cancer cells show increased dependence on glycolysis to produce ATP; a phenomenon known as the Warburg effect.[2] This metabolic alteration is a fundamental difference between cancer cells and normal cells, offering a therapeutic strategy to selectively kill cancer cells using glycolysis inhibitors (reviewed in ref 3). It has also been shown that glycolysis inhibitors induce cancer cell death more effectively in a hypoxic environment, which occurs within developing tumors.[4] Moreover, this hypoxic environment renders cancer cells less sensitive to other cancer drugs, such as cytarabine and doxorubicin.[4]

In our study presented herein, we screened for new small molecules that modulate the biochemical pathways facilitating cancer cell survival in hypoxic environments. A "hit" molecule from this screen was found to target enolase, which is a component of the glycolysis pathway. Our study describes the discovery and characterization of this hit molecule, which we have termed ENOblock (**1**). Subsequent analysis of ENOblock revealed roles for enolase in cancer progression and gluconeogenesis. To our knowledge, ENOblock is the first small molecule probe for enolase that is suitable for biological studies. In addition, ENOblock is an attractive candidate compound for pharmacokinetic and pharmacodynamic studies to assess its potential for drug development.

RESULTS AND DISCUSSION

Identification of AP-III-a4 (ENOblock). We developed a novel, dual screening system to identify molecules that preferentially kill cancer cells in a hypoxic environment (Figure

Received: December 14, 2012
Accepted: April 2, 2013
Published: April 2, 2013

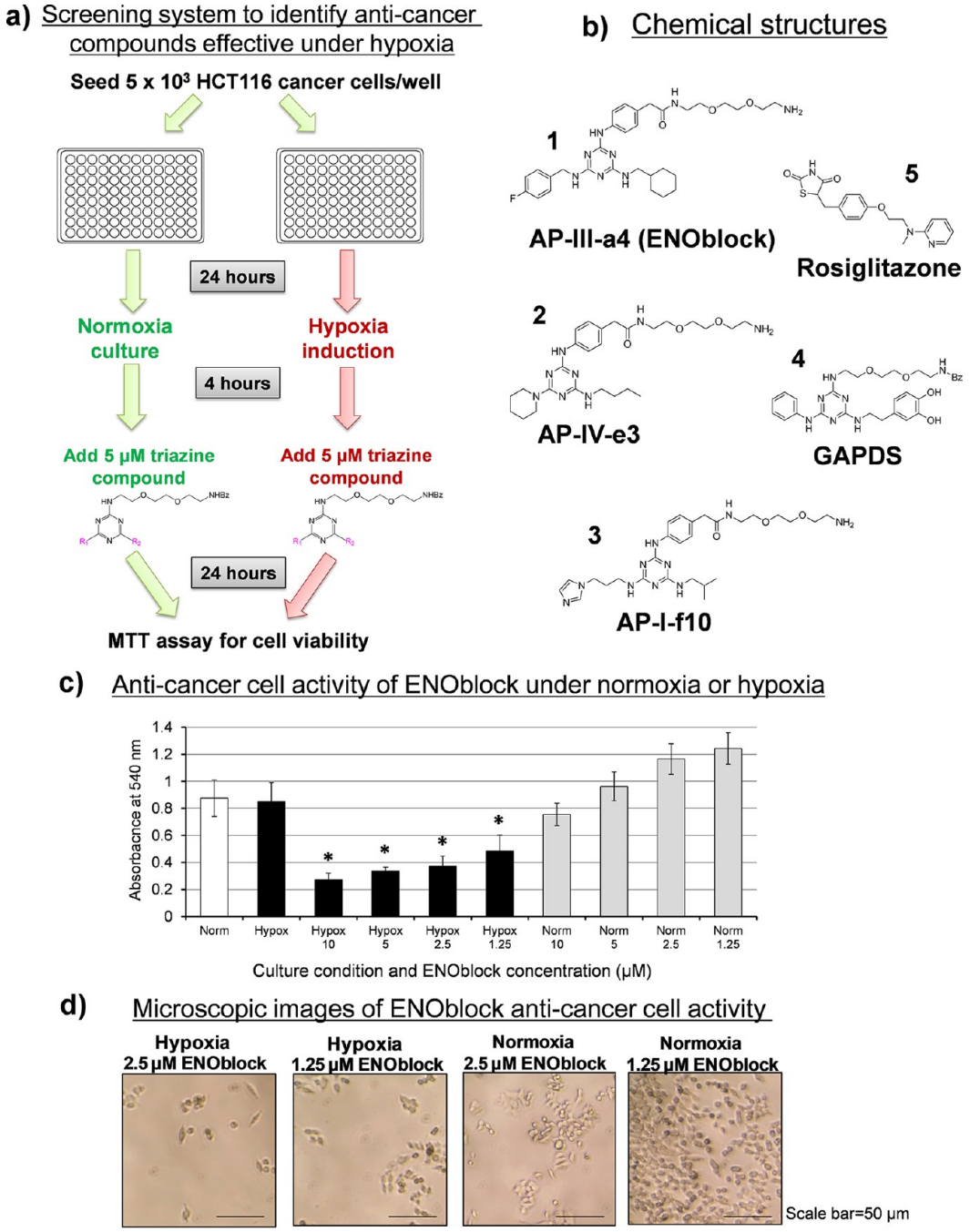

Figure 1. Discovery of compound AP-III-a4 (ENOblock). (a) Schematic of the screening system used to detect apoptosis inducers effective under hypoxia. HCT116 cancer cells were seeded in parallel 96-well culture plates. Hypoxia was induced in one plate using 150 μM cobalt chloride treatment. Triazine library compound at 5 μM concentration was added 4 h later, and cell death was determined 24 h after hypoxia induction. "Hit" compounds induced 25% or greater levels of cell death under hypoxia compared to normoxia (as measured by MTT assay absorbance). (b) Chemical structures of AP-III-a4 (ENOblock) and the control compounds, AP-IV-e3 and AP-I-f10. Chemical structures of GAPDS, which targets glyceraldehyde 3-phosphate dehydrogenase (GAPDH), and rosiglitazone, a well-known anti-diabetes drug, are also shown. (c) ENOblock induced higher levels of HCT116 colon cancer cell death in hypoxic conditions (Hypox) compared to normoxia (Norm). Error = SD; * = P value < 0.05 for increased cell death compared to normoxia. (d) Representative phase contrast microscopic images of HCT116 colon cancer cells treated with ENOblock under normoxia or hypoxia.

1, panel a). A small molecule library of 384 triazines prepared on a solid support[5] (Supplementary Scheme 1) was screened. Please note that compounds in this library have previously been shown to be cell permeable.[6] A "hit" molecule was defined as an inducer of at least 25% increased cancer cell toxicity in hypoxia compared to normoxia (as determined using the 3-(4,5-dimethylthiazol-2-yl)-2,5-diphenyltetrazolium bromide, a tetrazole (MTT) assay). Five from 384 triazines screened produced greater cancer cell toxicity under hypoxia. The best performing hit molecule was AP-III-a4 (**1**) (Figure 1, panel b). AP-III-a4 treatment of cancer cells cultured under hypoxia reduced cell viability dose-dependently (Figure 1, panels c,d). NMR and HRMS analytical data for compound AP-III-a4 is shown in Supplementary Figure 1 (panels a,b).

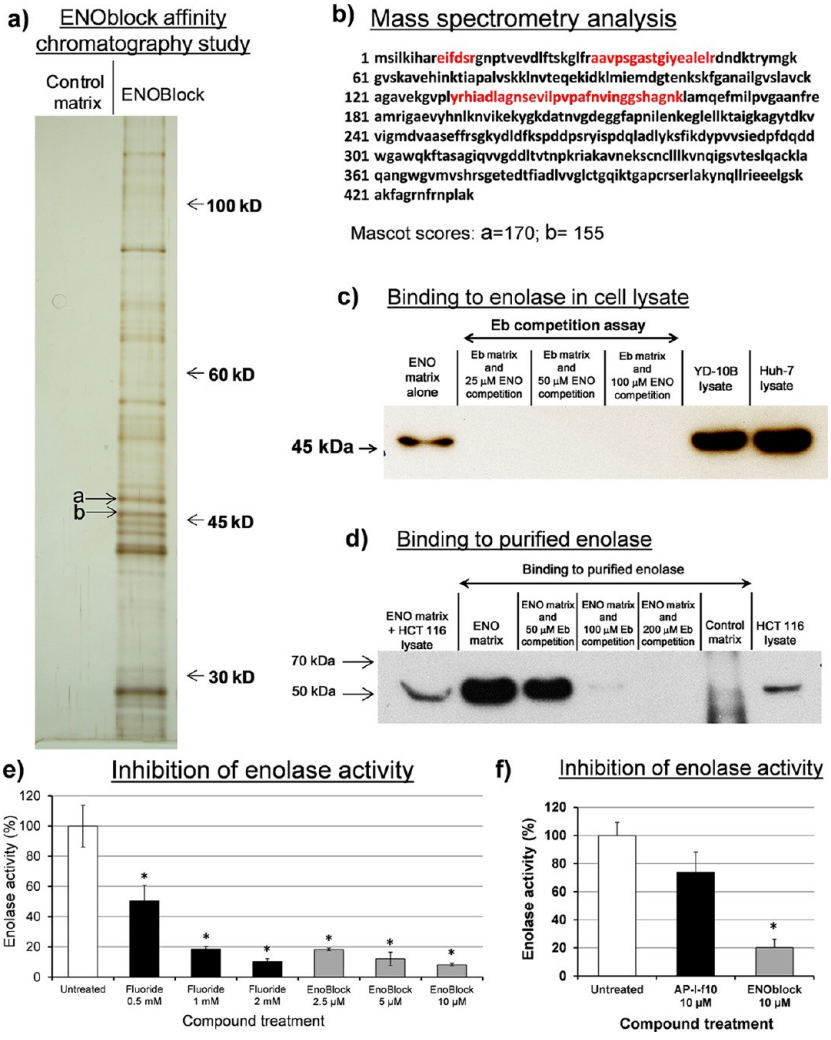

Figure 2. Discovery that compound AP-III-a4 (ENOblock) is a direct inhibitor of enolase. (a) Affinity chromatography study for ENOblock in HCT116 cancer cells. Protein bands marked "a" and "b" were identified by mass spectrometry as subunits of the heterodimer, enolase. In contrast, mass spectrometry failed to identify the other prominent protein bands in the eluate from the ENOblock affinity matrix. Control matrix = AP-IV-e3 (**2**) affinity matrix, which showed no binding to HCT116 lysate proteins. (b) Sequence identification for the enolase monomer subunit. Identified peptides are shown in red. Mascot scores above 100 were deemed to be significant. (c) Western blot analysis confirmed that enolase in HCT116 cancer cell lysate binds to the ENOblock affinity matrix. Competition analysis using free ENOblock (abbreviated as ENO) as a competitor completely inhibited enolase binding to the ENOblock affinity matrix. Twenty micrograms of cell lysate from YD-10B oral cancer cells or Huh7 hepatocytes were used as positive controls. (d) Western blot analysis confirmed that purified human enolase binds to the ENOblock affinity matrix. Competition analysis using free ENOblock as a competitor inhibited purified enolase binding to the ENOblock affinity matrix. In contrast, the AP-IV-e3 control compound affinity matrix could not bind to the purified enolase. As a positive control, ENOblock affinity matrix was incubated with 200 μg of HCT 116 cell lysate; 50 μg cell lysate from HCT116 cancer cells was used as a positive control for the enolase antibody. (e) ENOblock dose-dependently inhibited the activity of purified enolase. ENOblock inhibited enolase activity at a markedly lower concentration than the well-known enolase inhibitor, sodium fluoride (NaF); 2.5 μM ENOblock treatment reduced enolase activity to a level as approximated with 1 mM NaF treatment. Error = SD; * = $P < 0.05$ compared to the untreated group. (f) AP-I-f10, a "non-hit" compound from the same triazine library as ENOblock, did not significantly inhibit enolase activity. ENOblock was used as a positive control. Error = SD; * = $P < 0.05$ compared to the untreated group.

ENOblock Binds to Enolase and Inhibits Its Activity. Affinity chromatography was used to identify the cellular target for AP-III-a4. Target identification strategies for the triazine library used in this study are relatively straightforward, because the molecules contain a built-in linker moiety. This allows conjugation to an affinity matrix with reduced risk of compromising biological activity. Silver staining of proteins eluted from the AP-III-a4 affinity matrix is shown in Figure 2, panel a. Mass spectrometry analysis revealed that two protein bands of approximately 45 kD mass were subunits of enolase, a glycolysis enzyme, and a protein band of approximately 40 kD was actin (Figure 2, panel b; the entire mass spectrometry analysis for AP-III-a4 is shown in Supplementary Figure 2 and Supplementary Table 1). However, AP-III-a4 did not affect actin polymerization (Supplementary Figure 3), indicating that actin is not an active target. Thus, we renamed molecule AP-III-a4 "ENOblock". ENOblock binding to enolase in cancer cell lysates was confirmed by Western blot analysis of proteins eluted from the ENOblock affinity matrix. Competition analysis with free ENOblock inhibited enolase binding to the ENOblock affinity matrix (Figure 2, panel c). Moreover, ENOblock could bind to purified human enolase, suggesting a

dx.doi.org/10.1021/cb300687k | *ACS Chem. Biol.* 2013, 8, 1271−1282

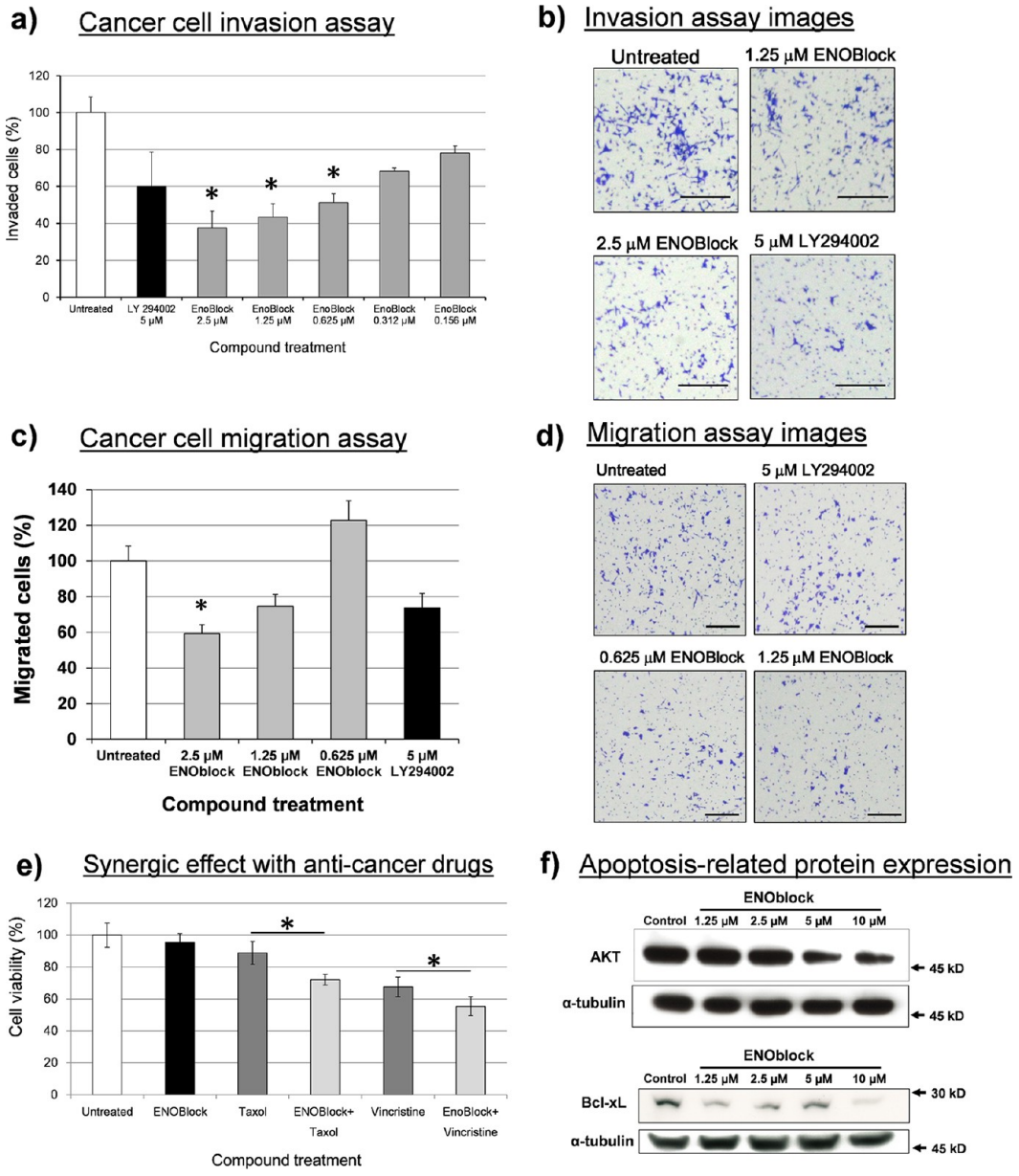

Figure 3. ENOblock can inhibit cancer cell invasion and migration. (a) ENOblock treatment of HCT116 cancer cells under normoxia inhibited invasion dose-dependently. ENOblock significantly inhibits cancer cell invasion at a treatment concentration of 0.625 μM (P value = 0.0481), whereas treatment with 5 μM LY294002 reduced cancer cell invasion, but without achieving statistical significance (P value = 0.27). Error = SD; * = $P < 0.05$ compared to the untreated group. (b) Microscopic images of crystal violet stained HCT116 cells invaded onto the transwell inserts (scale bar = 100 μm). (c) ENOblock treatment of HCT116 cancer cells under normoxia inhibited cell migration dose-dependently. Similar to cell invasion, ENOblock was more effective than LY294002 at inhibiting cell migration. Error = SD; * = $P < 0.05$ compared to the untreated group. (d) Microscopic images of crystal violet stained HCT116 cells migrated onto the transwell inserts (scale bar = 100 μm). (e) ENOblock treatment of HCT116 cancer cells increased sensitivity to the antitubulin chemotherapeutics taxol and vincristine. Cells were treated with 10 nM taxol and 10 nM vincristine, with or without 10 μM ENOblock. Error = SD; * = $P < 0.05$ between the groups indicated on the graph. (f) ENOblock treatment of HCT116 cancer cells decreased the expression of AKT and Bcl-Xl, which are negative regulators of apoptosis. For the AKT Western blot, cells were treated with ENOblock for 24 h; for the Bcl-Xl Western blot, cells were treated with ENOblock for 48 h.

direct interaction between ENOblock and enolase (Figure 2, panel d). Subsequent analysis showed that enolase activity can be inhibited by ENOblock dose-dependently (Figure 2, panel e; as an additional control, we also tested another non-hit compound from the tagged triazine library, AP-I-f10 (**3**), which was shown to not reduce enolase activity (Figure 2, panel f)). Further biochemical analysis showed that the half maximal inhibitory concentration (IC_{50}) of enolase inhibition by ENOblock is 0.576 μM (Supplementary Figure 4).The role of enolase in enhancing cancer cell survival under hypoxia was confirmed by siRNA-mediated knock-down of enolase expression (Supplementary Figure 5). To test that ENOblock treatment under hypoxia induced cytotoxicity, rather than inhibition of cell proliferation, cancer cells were stained with trypan blue (Supplementary Figure 6). ENOblock-treated cells showed increased trypan blue uptake under hypoxia, which confirmed the induction of cell death.

dx.doi.org/10.1021/cb300687k | *ACS Chem. Biol.* 2013, 8, 1271−1282

A) Toxicological analysis using zebrafish

Test Compound	Somite	Tail detachment	Otoliths	Eyes	Heart Beat	Circulation	Delayed Hatching	Skeletal deformities	Lack of swimming
Control	-	-	-	-	-	-	-	-	-
ENOblock(10μM)	-	-	-	-	-	-	-	-	-
ENOblock(20μM)	-	-	-	-	-	-	-	-	+
ENOblock(40μM)	+	-	-	-	-	+	-	+	+

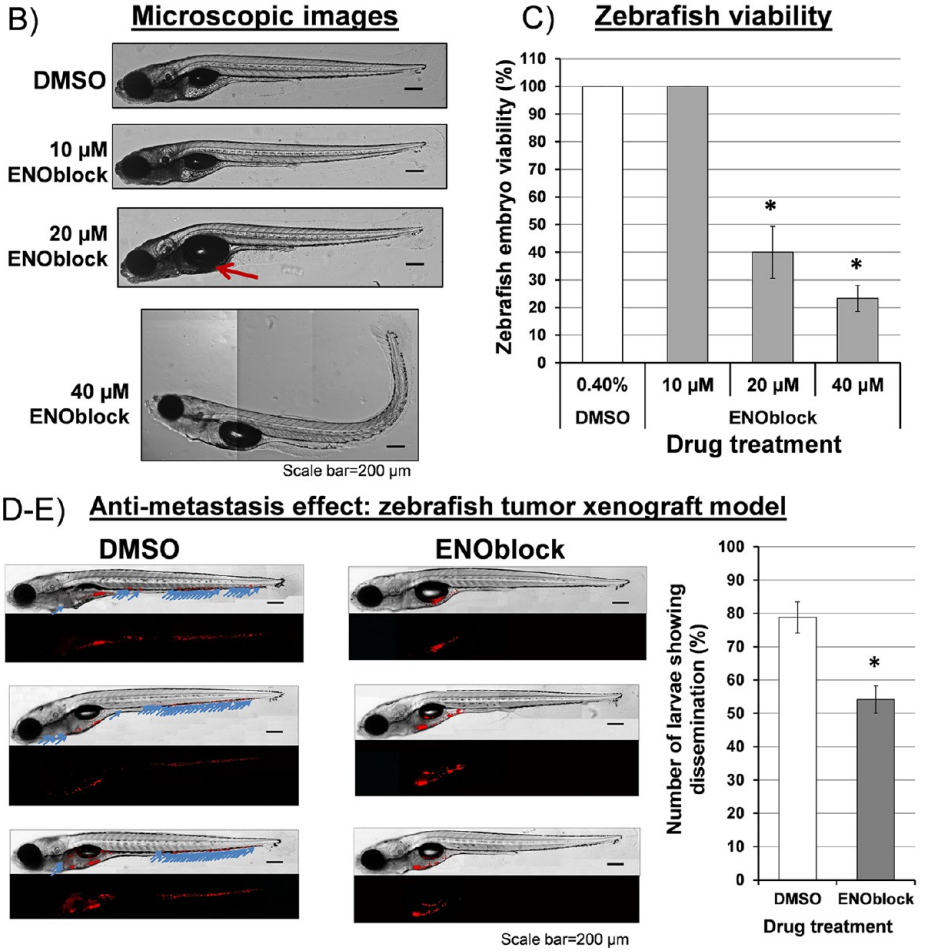

Figure 4. Toxicological study of ENOblock and *in vivo* analysis of anticancer activity. (A) Toxicological analysis of ENOblock treatment using the zebrafish larvae system. Assessment of various developmental parameters showed that a dose of 10 μM ENOblock could be tolerated by the larvae, but a dose of 20 μM ENOblock inhibited the ability to swim. (B) Microscopic assessment of 72 days post fertilization (dfp) zebrafish larvae exposed to increasing doses of ENOblock. It can be seen that a dose of 20 μM ENOblock produced an abnormally large swim bladder, as indicated by the red arrow. A dose of 40 μM ENOblock produced multiple abnormalities in the larvae. (C) Doses of 20 or 40 μM ENOblock also reduced overall zebrafish larvae viability, while a dose of 10 μM ENOblock did not affect viability. Error = SD; * = $P < 0.05$ compared to the DMSO treated group. (D,E) Treatment of HCT116-xenotransplanted zebrafish with a dose of 10 μM ENOblock for 96 h reduced the number of embryos showing migration and metastasis (distributed cancer cells) from the yolk sac injection site. DMSO treatment served as a control. Three representative embryos are shown from each experimental group, and distributed cancer cell foci are designated with blue arrows. Quantification of xenotransplanted cancer cell microfoci confirmed that ENOblock treatment significantly reduced cancer cell migration and metastasis. Error = SD; * = $P < 0.05$ compared to the DMSO-treated group.

ENOblock Inhibits Cancer Cell Migration and Invasion. Enolase is a "moonlighting" metabolic enzyme, because it performs multiple functions that are unrelated to its innate glycolytic function.[7,8] Thus, we speculated that ENOblock represents a powerful chemical tool to characterize the moonlighting functions of enolase. As our first test, we assessed the role of enolase in cancer progression (Figure 3). We found that enolase inhibition by ENOblock can reduce cancer cell invasion, which to our knowledge is the first confirmation that enolase activity is linked to metastasis (Figure 3, panels a,b; as an additional control, we also tested another compound from the tagged triazine library, AP-I-f10 (**3**), which did not reduce cell invasion (Supplementary Figure 7)). Moreover, ENOblock treatment also inhibited cancer cell migration (Figure 3, panels c,d). ENOblock treatment reduced cancer cell invasion/migration under normoxia at concentrations that do not induce cytotoxicity (compare Figures 3, panels a,b with Figure 1, panel c). Previous studies have shown that enolase expression knockdown can increase cytotoxicity induced by the cancer drugs taxol and vincristine.[9] In accordance with this finding, we observed that ENOblock treatment could also increase cancer cell cytotoxicity induced by taxol and vincristine (Figure 3,

dx.doi.org/10.1021/cb300687k | *ACS Chem. Biol.* 2013, 8, 1271−1282

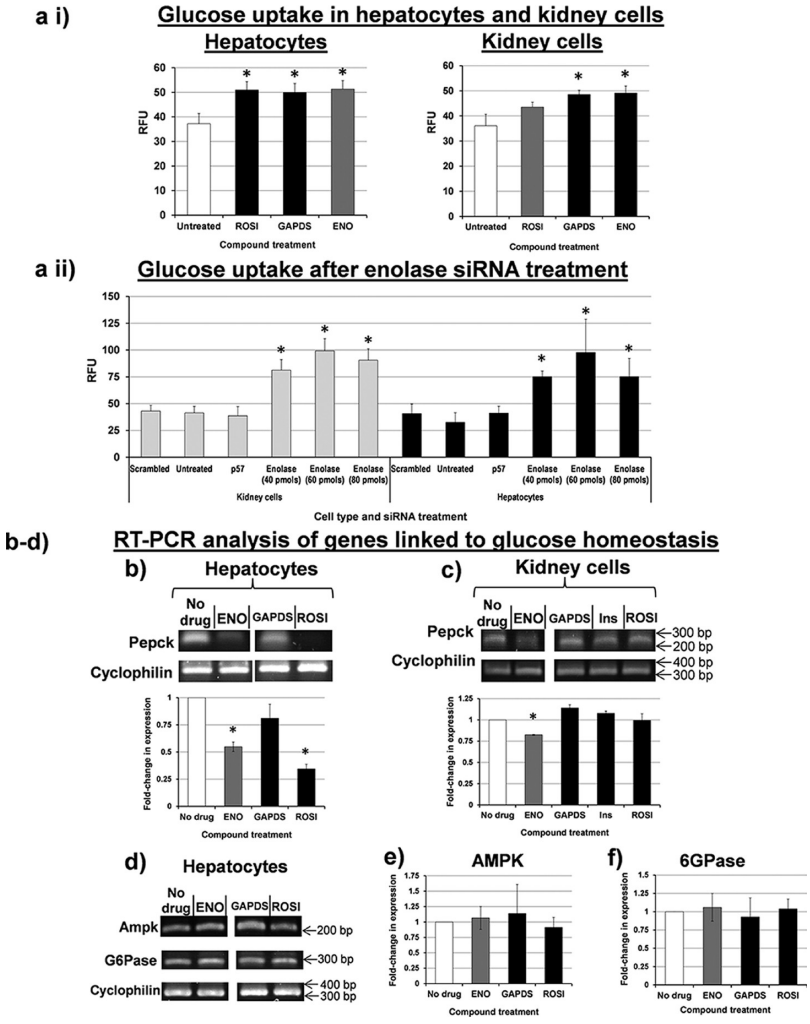

Figure 5. ENOblock can induce glucose uptake and inhibit phosphoenolpyruvate carboxykinase (PEPCK) expression. (a i) Ten micromolar ENOblock (abbreviated as ENO) treatment of Huh7 hepatocytes or HEK kidney cells for 24 h induced glucose uptake, as measured using the fluorescent glucose probe, 2-NBDG. Twenty-four hour treatment with 10 μM GAPDS, a small molecule modulator of the glycolytic enzyme GAPDH, could also induce glucose uptake in the hepatocytes. In contrast, 24 h treatment with 10 μM rosiglitazone (abbreviated as ROSI), a well-known anti-diabetes drug, could induce glucose uptake in hepatocytes, but not kidney cells. Error = SD; * = $P < 0.05$ compared to the untreated group. (a ii) siRNA-mediated knockdown of enolase expression in hepatocytes or kidney cells induced glucose uptake, as shown by increased labeling with the fluorescent glucose probe, 2-NBDG. Cells were treated with increasing concentrations of enolase (ENO1) siRNA or two types of negative control siRNA: (1) 80 pmols scrambled or (2) 80 pmols p57 (a cyclin dependent kinase inhibitor). Twenty-four hours post-transfection with siRNA, cells transferred to a 96-well culture plate at a density of 10^4 cells/well and, 24 h later, treated with 100 μM 2-NBDG for 30 min. 2-NBDG fluorescence was then measured as described in Methods. Error = SD; * = $P < 0.05$ for increased glucose uptake compared to cells treated with scrambled siRNA. (b) Ten micromolar ENOblock treatment of Huh7 hepatocytes for 24 h inhibited expression of PEPCK, a key positive regulator of gluconeogenesis. Twenty-four hour treatment with 10 μM rosiglitazone could also inhibit PEPCK expression. However, 24 h treatment with 10 μM GAPDS did not inhibit PEPCK expression. Error = SD; * = $P < 0.05$ compared to the no drug (DMSO-treated) group. (c) Ten micromolar ENOblock treatment of HEK cells for 24 h inhibited expression of PEPCK. In contrast, treatment with 10 μM GAPDS, 1 μg/mL insulin (abbreviated as Ins), or 10 μM rosiglitazone for 24 h did not reduce PEPCK expression. Error = SD; * = $P < 0.05$ for reduced PEPCK expression compared to the no drug (DMSO-treated) group. (d–f) Ten micromolar ENOblock treatment of hepatocytes for 24 h did not affect expression of the enzymes glucose 6-phosphatase (G6 Pase), which also regulates gluconeogenesis, or 5′ AMP-activated protein kinase (AMPK), which regulates cellular energy homeostasis. Similarly, 24 h treatment with either 10 μM GAPDS or 10 μM rosiglitazone for 24 h did not affect the expression of these enzymes (Error bar = SD).

panel e). To investigate how ENOblock may induce cancer cell cytotoxicity, we measured the expression of two proteins that are linked to the induction of apoptosis, AKT[10] and Bcl-xL.[11] ENOblock treatment decreased the expression of AKT and Bcl-xL (Figure 3, panel f). AKT and Bcl-xL are both target proteins for cellular responses to hypoxia.[12,13] Thus, it can be speculated that down-regulation of AKT and Bcl-xL expression by ENOblock reduces the ability of cells to adapt to the hypoxic condition.

The zebrafish (*Danio rerio*) cancer cell xenograft model is gaining increasing research prominence as a validated, convenient tool for testing candidate cancer drugs *in vivo*.[14] In addition, zebrafish is a relevant vertebrate platform for predicting toxicological effects in mammals.[15] We observed that 10 μM ENOblock treatment of developing zebrafish larvae was nontoxic (Figure 4, panels A–C). Employing a recently published zebrafish tumor xenograft model validated for anticancer drug testing,[14,16] we observed that ENOblock

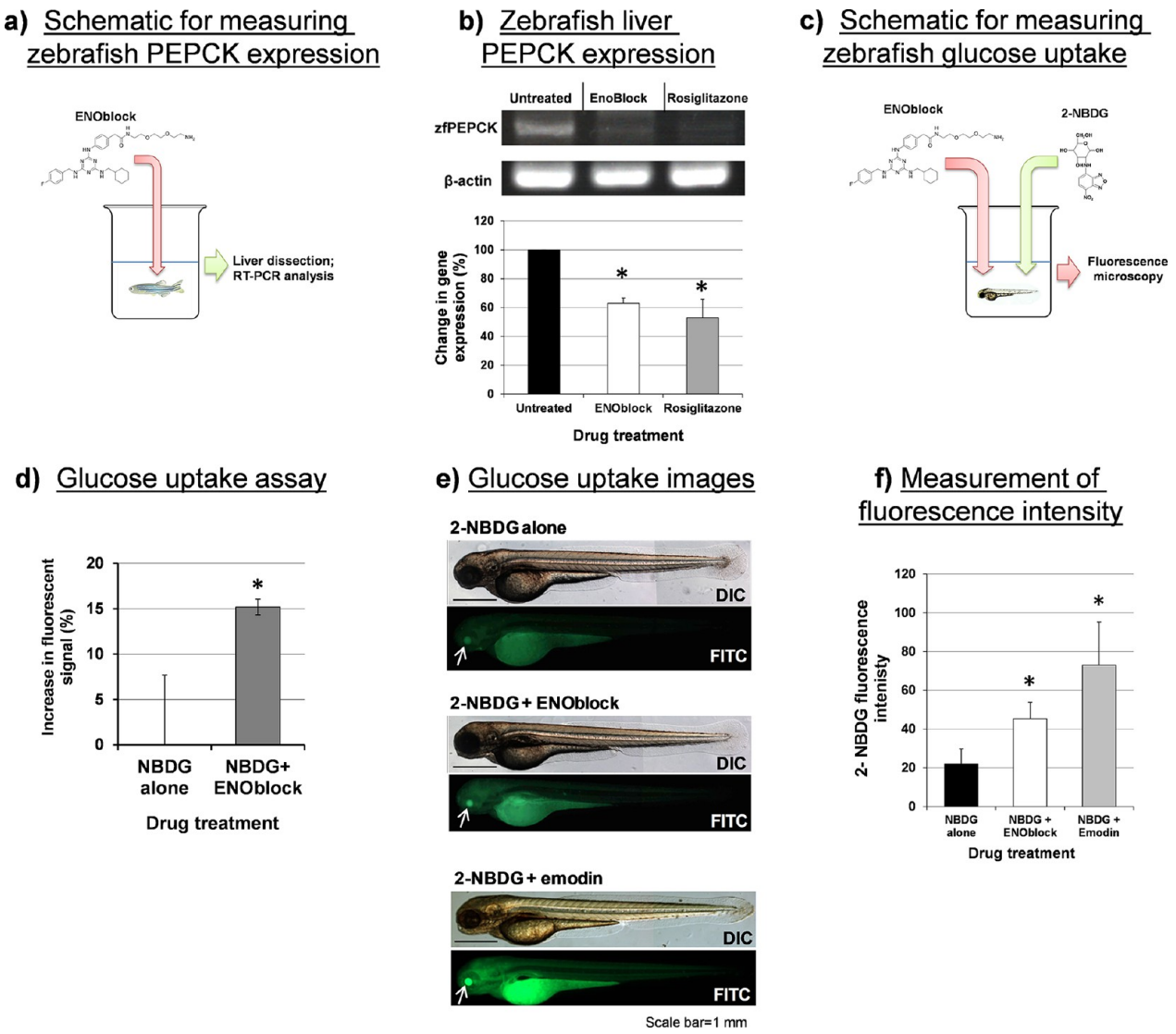

Figure 6. ENOblock can inhibit PEPCK expression and induce glucose uptake *in vivo*. (a) Schematic of our approach to measure the effect of ENOblock treatment on PEPCK in zebrafish. (b) Three hour treatment with a dose of 10 μM ENOblock inhibited PEPCK expression in adult zebrafish liver. Three hour treatment with 10 μM rosiglitazone, which inhibited PEPCK expression in hepatocytes, also inhibited PEPCK expression in the zebrafish liver. Error = SD; * = $P < 0.05$ compared to the untreated group. (c) Schematic of our approach to measure uptake of a fluorescent-tagged glucose bioprobe (2-NBDG) in zebrafish larvae, which can be imaged due to their transparency. (d) Treatment of 72 hpf zebrafish with 10 mM ENOblock for 1 h induced glucose uptake, as assessed by fluorescent plate reader measurement of the 2-NBDG signal in lysed larvae (Error = SD; * = $P < 0.05$). (e) Four hours treatment with a dose of 10 μM ENOblock increased glucose uptake in the zebrafish larvae. Increased glucose uptake can be observed throughout the developing embryo and, especially, in the eye (indicated by the white arrow), intestine, and yolk sac. As a comparison, zebrafish treated with 10 μg/mL emodin, a known anti-diabetic natural product that promotes glucose uptake, also showed enhanced glucose uptake in a similar but more intense pattern compared to the zebrafish treated with ENOblock. (f) Quantification of fluorescence signal intensity from the fluorescent glucose probe 2-NBDG in the eye of the 72 hpf zebrafish larvae, which is known to express numerous glucose transporters at this stage of development. Four hour treatment of the larvae with a dose of 10 μM ENOblock or 10 μg/mL emodin induced significantly greater fluorescent tagged glucose uptake in the zebrafish eye. Error = SD; * = $P < 0.05$ compared to the zebrafish treated with 2-NBDG alone.

treatment reduced cancer cell dissemination, suggesting an inhibition of cancer cell migration and invasion processes (Figure 4, panels D,E).

ENOblock Induces Cellular Glucose Uptake and Down-regulates PEPCK Expression. Interestingly, ENOblock (compound AP-III-a4) was among a group of triazines previously identified in a screen to discover novel modulators of glucose uptake,[17] although the mechanism of action was not characterized in that study. Thus, we confirmed the ability of ENOblock to increase glucose uptake in cells, using the fluorescent probe 2-(*N*-(7-nitrobenz-2-oxa-1,3-diazol-4-yl)-amino)-2-deoxyglucose (2-NBDG), which can be used to monitor cellular glucose flux[18,19] (Figure 5, panel a i). To our knowledge, this is the first demonstration that modulation of enolase function is linked to increased glucose uptake. The role of enolase in promoting cellular glucose uptake was confirmed by siRNA-mediated knock-down of enolase expression (Figure 5, panel a ii).

To characterize the mechanism by which ENOblock promotes glucose uptake, we assessed the expression of key enzymes linked to glucose homeostasis. We found that ENOblock down-regulates the expression of phosphoenolpyr-

dx.doi.org/10.1021/cb300687k | *ACS Chem. Biol.* 2013, 8, 1271–1282

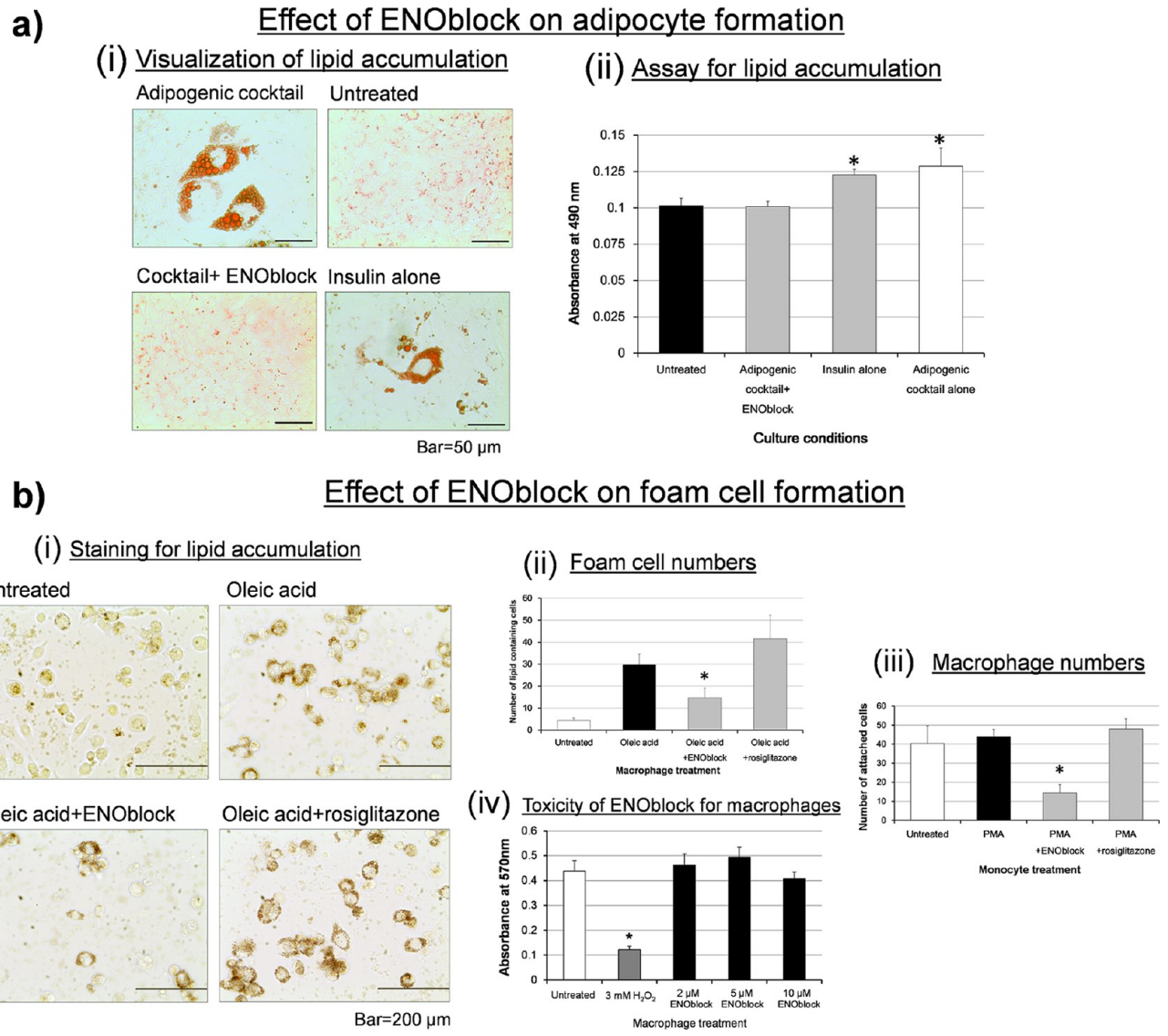

Figure 7. ENOblock inhibits adipogenesis and foam cell formation. (a) (i) Microscopic analysis of pre-adipocytes undergoing adipogenesis showed that treatment with 10 μM ENOblock inhibited lipid accumulation, as shown by an absence of Oil Red O staining. In contrast, treatment of pre-adipocytes with insulin, without adipogenesis-inducing factors, still induced lipid accumulation. (a) (ii) Quantification of lipid accumulation confirmed that ENOblock treatment blocked lipid accumulation during adipogenesis. Error = SD; * = $P < 0.05$ compared to untreated adipocytes. (b) (i) Microscopic analysis of macrophages treated with oleic acid showed that treatment with 10 μM ENOblock inhibited foam cell formation, as shown by reduced Oil Red O staining. (b) (ii) Confirmation that 10 μM ENOblock inhibited foam cell formation, as assessed by counting cells that showed lipid accumulation. In contrast, macrophage treatment with the anti-diabetes drug rosiglitazone (10 μM) during development into foam cells did not affect the number of cells showing lipid accumulation. Error = SD; * = $P < 0.05$ for reduced lipid-containing cells compared to the oleic acid treated group adipocytes. (b) (iii) Treatment of monocytes with 10 μM ENOblock inhibited differentiation into macrophages, as assessed by counting the number of cells attached to the culture dish. In contrast, monocyte treatment with 10 μM rosiglitazone did not affect differentiation into macrophages. Error = SD; * = $P < 0.05$ for reduced numbers of attached cells compared to the phorbol 12-myristate 13-acetate (PMA) treated group. (b) (iv) The effects of ENOblock treatment on macrophages was not due to cytotoxicity, as shown by MTT assay analysis. Treatment with 3 mM H_2O_2 for 48 h was used as a positive control. Error = SD; * = $P < 0.05$ for reduced absorbance (570 nm) compared to the untreated group.

uvate carboxykinase (PEPCK) in hepatocytes, which catalyzes the rate-limiting step of liver tissue gluconeogenesis,[20] the process whereby glucose is synthesized (Figure 5, panel b). Of note, there is a precedent for the finding that small molecule regulation of a glycolysis enzyme regulates glucose uptake, with the report that GAPDS (**4**) targets glyceraldehyde 3-phosphate dehydrogenase (GAPDH) to promote glucose uptake (GAPDH catalyzes the sixth step of glycolysis, upstream of enolase).[21] Thus, we also measured PEPCK expression in hepatocytes after treatment with GAPDS or rosiglitazone (**5**), a well-known diabetes drug that can down-regulate PEPCK expression.[22] It was found that rosiglitazone can down-regulate PEPCK expression, while GAPDS had no effect, suggesting that GAPDS and ENOblock promote glucose uptake by different cellular mechanisms (Figure 5, panel b). Interestingly, the kidney is also a site of gluconeogenesis,[23] and it was observed that ENOblock treatment could also down-regulate PEPCK expression in kidney cells (Figure 5, panel c). In contrast, treatment of kidney cells with GAPDS, rosiglitazone, or insulin did not affect PEPCK expression (Figure 5, panel c). The ability of ENOblock to inhibit PEPCK protein expression in hepatocytes and kidney cells was confirmed by Western

blotting analysis (Supplementary Figure 8). The enzyme glucose 6-phosphatase (G6 Pase) catalyzes the final step in gluconeogenesis plays a key role in the homeostatic regulation of glucose uptake by the liver.[24] We observed that ENOblock treatment of hepatocytes did not influence G6 Pase expression, which was also observed after treatment with GAPDS or rosiglitazone (Figure 5, panel d). The enzyme 5′ AMP-activated protein kinase (AMPK) plays a key role in cellular energy homeostasis.[25] Similar to G6 Pase, we observed that treatment of hepatocytes with ENOblock, GAPDS, or rosiglitazone did not affect AMPK expression (Figure 5, panels d–f).

ENOblock Down-regulates PEPCK Expression and Induces Glucose Uptake *in Vivo*. To investigate the effects of ENOblock on glucose homeostasis *in vivo*, we selected the zebrafish, because this animal model provides a convenient, rapid experimental format requiring small amounts of test compound. Moreover, it has been shown that zebrafish and mammals share similar glucose regulatory responses.[22] Adult zebrafish treated with ENOblock or rosiglitazone showed down-regulated hepatic PEPCK expression (Figure 6, panels a,b), which confirmed our cell-based findings. The fluorescent glucose probe 2-NBDG has been used to assess glucose uptake in zebrafish larvae, which are transparent and allow visualization of 2-NBDG fluorescence (e.g., ref 26). We observed that ENOblock treatment induced glucose uptake in zebrafish larvae (Figure 6, panels c–e). As a comparison, we also tested the effect of emodin (6-methyl-1,3,8-trihydroxyanthraquinone, a biologically active plant constituent that is known to promote cellular glucose uptake[27]). 2-NBDG fluorescent signal in lysed larvae was measured using a fluorescent plate reader (Figure 6, panel d). Results from this approach confirmed that ENOblock treatment induced glucose uptake *in vivo*. Fluorescence microscopy analysis of 2-NBDG treated larvae showed that emodin treatment increased glucose uptake (Figure 6, panel e). 2-NBDG uptake was quantified by measuring 2-NBDG fluorescence intensity in the zebrafish larvae eye at 72 hpf, because this tissue has been show to express a relatively large number of glucose transporter isoforms at this stage of development.[28] Image J anaylsis (National Institutes of Health, USA) confirmed that ENOblock or emodin treatment could promote glucose uptake in the zebrafish.

ENOblock Treatment Inhibits Adipogenesis and Foam Cell Formation. Commonly prescribed drugs for patients with diabetes are associated with side effects, such as weight gain or cardiovascular events.[29] Thus, we tested the effect of ENOblock on lipid accumulation in differentiating adipocyte precursor cells, which provides a convenient test for novel anti-obesity agents.[30] The positive effect of rosiglitazone on adipogenesis has already been described.[31] In contrast, we observed that ENOblock treatment inhibited lipid accumulation in adipocyte precursor cells exposed to adipogenic factors (Figure 7, panel a). Foam cell differentiation from macrophages adhered to blood vessel walls is a crucial step in the progression of atherosclerosis.[32] ENOblock treatment inhibited lipid accumulation in macrophages induced to undergo foam cell differentiation (Figure 7, panel b(i)). Cell counting showed that ENOblock treatment inhibited both foam cell differentiation from macrophages and macrophage differentiation from monocytes (Figure 7, panel b(ii,iii)). These inhibitory effects of ENOblock were observed at treatment concentrations that did not induce cytotoxicity (Figure 7, panel b(iv)).

In this study, we describe a new small molecule, ENOblock, which is the first nonsubstrate analogue that directly binds to enolase and can be used as a probe to characterize enolase activity in biological systems. Enolase is a metalloenzyme that catalyzes the dehydration of 2-phospho-D-glycerate to phosphoenolpyruvate, which is the ninth and penultimate step of glycolysis.[7] Enolase also performs multiple functions that are unrelated to its innate glycolytic function.[1,7] To our knowledge, small molecule tools to clarify the diverse roles of enolase are rare. The most widely reported enolase inhibitor is phosphonoacetohydroxamate (PhAH). PhAH is thought to mimic the aci-carboxylate form of the intermediate carbanion in the reaction and is only applicable for crystallographic studies (e.g., ref 33). Another two substrate analogues were developed, but these were only applied for direct spectrophotometric titration of the enolase active site and stopped-flow studies of enzyme kinetics (D-tartronate semialdehyde phosphate[34] and 3-aminoenolpyruvate phosphate[35]). Moreover, these substrate analogues are not commercially available. Inorganic sodium fluoride is also a substrate competitor for enolase. However, fluoride is not suitable for studying enolase in biological systems due to a variety of nonspecific toxic effects, such as phosphatase inhibition and the induction of increased oxidative stress or perturbed antioxidant defense mechanisms.[36,37] A recent report described the malaria drug mefloquine as an enolase inhibitor in *Schistosoma mansoni*.[37] However, mefloquine could not directly bind to recombinant enolase from this parasite and could not inhibit purified enolase activity. This suggests that, unlike ENOblock, mefloquine may not bind to enolase directly but exerts its effects via interacting with an uncharacterized enolase-modulating molecule in the cell extract. For example, it has been shown that enolase can bind to vacuoles or form large macromolecular complexes associated with mitochondria.[37] Thus, we propose that ENOblock is a powerful chemical tool to characterize the various, non-glycolytic 'moonlighting'[38] functions of enolase.

When discussing the activity of ENOblock, we believe that it is important to differentiate between the effects of this compound in hypoxic or normoxic conditions. We discovered ENOblock by screening for compounds that can induce greater levels of cancer cell death under hypoxia compared to normoxia. We adopted this approach because common cancer chemotherapy drugs are less effective under hypoxia.[4] Our demonstration that enolase expression is rapidly up-regulated after the onset of hypoxia (Supplementary Figure 5) links the ability of ENOblock to kill cancer cells under hypoxia and its enolase inhibitory activity. Moreover, cancer cells are characterized by the Warburg effect, which is a group of metabolic alterations that increase reliance on anaerobic glycolysis for energy generation.[2] Thus, glycolysis inhibitors, such as 3-bromopyruvate and 6-aminonicotinamide, can kill cancer cells (reviewed in ref 3). In our study, we have shown that ENOblock selectively kills cancer cells under hypoxia (Figure 1, panels c,d), which is due to the glycolysis-related function of enolase (Supplementary Figure 5).

The multifunctional roles of enolase can also be probed using ENOblock under normoxia. For example, enolase is exported to the eukaryote cell surface via a nonclassical export pathway, and it has been suggested that enolase can mediate cancer cell invasion leading to metastasis.[39–40] We observed that ENOblock treatment of cancer cells under normoxia, at concentrations that are noncytotoxic, inhibited cancer cell invasion and migration (Figure 3, panels a–d). This finding suggests that

ENOblock can also target cell-surface-bound enolase to modulate cancer cell metastasis. Our *in vivo* analysis of ENOblock treatment on metastasis was also carried out under normoxia, which showed that ENOblock can prevent cancer cell metastasis without noticeably affecting cancer cell viability (Figure 4, panels d,e; the cancer cells appear to be retained at the injection site without any reduction in cell numbers). Moreover, enolase has been shown to be associated with the cell microtubule system, which may negatively affect the efficacy of cancer drugs that disrupt microtubules.[9,41] Our results show that ENOblock treatment can increase the ability of microtubule-destabilizing drugs to kill cancer cells (Figure 3, panel e). Therefore, we speculate that ENOblock warrants further studies to assess its potential as a drug candidate for cancer therapy, because it can inhibit cancer cell metastasis and synergize with microtubule-destabilizing drugs under normoxia, while also possessing the potential to selectively kill cancer cells in hypoxic niches within tumors (cancer stem cells have been shown to express hypoxia-inducible factors that promote their survival under hypoxia (reviewed in ref 42)).

Our study has also shown that enolase inhibition by ENOblock can induce cellular glucose uptake (Figure 5, panel a i). Our results indicate that the ability of ENOblock to increase glucose uptake is due to a reduction of PEPCK expression. PEPCK expression has also been shown to be inhibited by insulin.[43] PEPCK inhibition in the liver reduces gluconeogenesis and concomitantly promotes glucose uptake.[20,44] Interestingly, gluconeogenesis in the kidney also plays a significant role in regulating blood glucose levels,[23] and our results show that ENOblock, but not insulin or the diabetes drug, rosiglitazone, can inhibit PEPCK expression in kidney cells (Figure 5, panel c). In addition, we have shown that enolase knock-down by siRNA can also induce glucose uptake (Figure 5, panel b). However, it should be noted that treatment with enolase siRNA induced a greater degree of glucose uptake compared to treatment with ENOblock (compare Figures 5, panel a i and ii). Thus, we cannot discount the possibility that ENOblock may only have a weak effect on this particular aspect of enolase function to induce glucose uptake. However, our data also showed that ENOblock treatment of hepatocytes induced glucose uptake to a similar degree as the anti-diabetes drug rosiglitazone and GAPDS (which modulates GAPDH to induce glucose uptake[21]).

Our demonstration that ENOblock treatment can inhibit PEPCK expression *in vivo* and induce glucose uptake suggests that ENOblock may be suitable for further studies to assess its potential as an anti-diabetes drug candidate. In support of this, is can be noted that enolase expression is increased in diabetic patients compared to normal subjects.[45] Moreover, our results suggest that ENOblock inhibits some of the complications associated with the use of diabetes drugs, such as increased adipogenesis and foam cell formation (Figure 7). Insulin signaling is linked to accelerated foam cell formation,[46] and commonly prescribed diabetes drugs can induce adipogenesis or weight gain.[31] We believe that the ability of ENOblock to inhibit foam cell formation or adipogenesis further supports the potential of ENOblock to be developed as an anti-diabetic drug candidate. Interestingly, the most commonly prescribed anti-diabetic drug, metformin, also inhibits hepatic gluconeogenesis and is currently the subject of various clinical trials as an anticancer drug (reviewed in ref 47).

To our knowledge, this study provides the first link between enolase inhibition and down-regulation of PEPCK expression, which inhibits gluconeogenesis. However, a precedent for this relationship exists in Nature. Studies in the mold *Aspergillus nidulans* have shown that, unexpectedly, mutation of the *acuN* gene (which encodes enolase) induces growth inhibition on gluconeogenic but not glycolytic carbon sources.[48] Therefore, we believe that further studies are warranted to assess the possible regulatory roles that other glycolysis enzymes exert over gluconeogenesis in mammals.

The *in vivo* analyses of ENOblock treatment presented herein have utilized the zebrafish vertebrate model. Zebrafish possess considerable advantages as the primary animal for testing novel therapeutic agents, such as glucose homeostatic mechanisms that are conserved in mammals, the availability of a validated cancer drug testing system, and toxicological responses that correlate with mammalian tests.[14,15,22,49,50] Moreover, relatively small amounts of test compound are required. In addition, highly detailed studies of mammalian cell behavior can be carried out in zebrafish (e.g. ref 51). Therefore, we believe that our series of zebrafish-based analyses are a suitable format for the first report of ENOblock activity.

In summary, our study reports the small molecule ENOblock, which is the first nonsubstrate analogue inhibitor that directly binds to enolase and can be used to probe the various nonglycolytic functions of this enzyme. We have utilized ENOblock to assess the effect of enolase inhibition on cancer progression and show for the first time that enolase inhibition can reduce cancer cell metastasis *in vivo*. We also show for the first time that enolase inhibition can suppress the gluconeogenesis regulator PEPCK and is a new target for developing antidiabetic drugs. We believe that the discovery of ENOblock is a testament to the power of forward chemical genetics to provide new chemical probes, drug targets, and candidate therapeutics for previously uncharacterized cellular mechanisms regulating human disease. In light of the potential role of enolase in the pathogenesis of bacterial infections (such as *Yersinia pestis*, *Borrelia* spp., and *Streptococcus pneumonia*) and trypanosomatid parasites (reviewed in ref 52), in addition to the need to discover new glycolysis inhibitors for cancer therapy,[3] we believe that ENOblock has the potential to make significant contributions to our understanding of these disorders.

METHODS

A description of the following experimental methods can be found in the Supporting Information accompanying this manuscript: reagents and antibodies, cell culture conditions, construction of the tagged triazine library, screening for apoptosis inducers that maintain effectiveness under hypoxia, cell proliferation assay, small molecule target identification using affinity chromatography, actin polymerization assay, enolase activity assay, Western blot analysis, zebrafish tumor cell xenograft model, siRNA-mediated gene silencing, reverse transcription polymerase chain reaction analysis of mRNA expression, cancer cell invasion assay and migration assay, zebrafish care and maintenance, RNA isolation from drug-treated zebrafish, toxicological assessment of ENOblock, measurement of cellular glucose uptake, measurement of glucose uptake in zebrafish, induction and quantification of adipocyte formation, induction of macrophage foam cells, and statistics.

ASSOCIATED CONTENT

Supporting Information

This material is available free of charge via the Internet at http://pubs.acs.org.

AUTHOR INFORMATION

Corresponding Author

*E-mail: darren@gist.ac.kr.

Author Contributions

[‖]These authors contributed equally to this work.

Notes

The authors declare no competing financial interest.

ACKNOWLEDGMENTS

This research was supported by two grants from the National Research Foundation funded by the Korean government (MEST basic science research program (NRF-2012003460) to D.R.W. and MEST basic science research program (NRF-2012000462) to D.-W.J.).

REFERENCES

(1) Kim, J. W., and Dang, C. V. (2005) Multifaceted roles of glycolytic enzymes. *Trends Biochem. Sci. 30*, 142−150.

(2) Warburg, O., Wind, F., and Negelein, E. (1927) The metabolism of tumors in the body. *J. Gen. Physiol. 8*, 519−530.

(3) Pelicano, H., Martin, D. S., Xu, R. H., and Huang, P. (2006) Glycolysis inhibition for anticancer treatment. *Oncogene 25*, 4633−4646.

(4) Xu, R. H., Pelicano, H., Zhou, Y., Carew, J. S., Feng, L., Bhalla, K. N., Keating, M. J., and Huang, P. (2005) Inhibition of glycolysis in cancer cells: a novel strategy to overcome drug resistance associated with mitochondrial respiratory defect and hypoxia. *Cancer Res. 65*, 613−621.

(5) Khersonsky, S. M., Jung, D. W., Kang, T. W., Walsh, D. P., Moon, H. S., Jo, H., Jacobson, E. M., Shetty, V., Neubert, T. A., and Chang, Y. T. (2003) Facilitated forward chemical genetics using a tagged triazine library and zebrafish embryo screening. *J. Am. Chem. Soc. 125*, 11804−11805.

(6) Lee, L. L., Ha, H., Chang, Y. T., and DeLisa, M. P. (2009) Discovery of amyloid-beta aggregation inhibitors using an engineered assay for intracellular protein folding and solubility. *Protein Sci. 18*, 277−286.

(7) Pancholi, V. (2001) Multifunctional alpha-enolase: its role in diseases. *Cell. Mol. Life Sci. 58*, 902−920.

(8) Jeffery, C. J. (2009) Moonlighting proteins—an update. *Mol. Biosyst. 5*, 345−350.

(9) Georges, E., Bonneau, A. M., and Prinos, P. (2011) RNAi-mediated knockdown of alpha-enolase increases the sensitivity of tumor cells to antitubulin chemotherapeutics. *Int. J. Biochem. Mol. Biol. 2*, 303−308.

(10) Kauffmann-Zeh, A., Rodriguez-Viciana, P., Ulrich, E., Gilbert, C., Coffer, P., Downward, J., and Evan, G. (1997) Suppression of c-Myc-induced apoptosis by Ras signalling through PI(3)K and PKB. *Nature 385*, 544−548.

(11) Boise, L. H., Gonzalez-Garcia, M., Postema, C. E., Ding, L., Lindsten, T., Turka, L. A., Mao, X., Nunez, G., and Thompson, C. B. (1993) bcl-x, a bcl-2-related gene that functions as a dominant regulator of apoptotic cell death. *Cell 74*, 597−608.

(12) Alvarez-Tejado, M., Naranjo-Suarez, S., Jimenez, C., Carrera, A. C., Landazuri, M. O., and del Peso, L. (2001) Hypoxia induces the activation of the phosphatidylinositol 3-kinase/Akt cell survival pathway in PC12 cells: protective role in apoptosis. *J. Biol. Chem. 276*, 22368−22374.

(13) Chen, N., Chen, X., Huang, R., Zeng, H., Gong, J., Meng, W., Lu, Y., Zhao, F., Wang, L., and Zhou, Q. (2009) BCL-xL is a target gene regulated by hypoxia-inducible factor-1{alpha}. *J. Biol. Chem. 284*, 10004−10012.

(14) Jung, D. W., Oh, E. S., Park, S. H., Chang, Y. T., Kim, C. H., Choi, S. Y., and Williams, D. R. (2012) A novel zebrafish human tumor xenograft model validated for anti-cancer drug screening. *Mol. Biosyst. 8*, 1930−1939.

(15) Sipes, N. S., Padilla, S., and Knudsen, T. B. (2011) Zebrafish: as an integrative model for twenty-first century toxicity testing. *Birth Defects Res., Part C 93*, 256−267.

(16) Jung, D. W., Kim, J., Che, Z. M., Oh, E. S., Kim, G., Eom, S. H., Im, S. H., Ha, H. H., Chang, Y. T., and Williams, D. R. (2011) A triazine compound S06 inhibits proinvasive crosstalk between carcinoma cells and stromal fibroblasts via binding to heat shock protein 90. *Chem. Biol. 18*, 1581−1590.

(17) Jung, D. W., Ha, H. H., Zheng, X., Chang, Y. T., and Williams, D. R. (2011) Novel use of fluorescent glucose analogues to identify a new class of triazine-based insulin mimetics possessing useful secondary effects. *Mol. Biosyst. 7*, 346−358.

(18) Kim, W. H., Lee, J., Jung, D. W., and Williams, D. R. (2012) Visualizing sweetness: increasingly diverse applications for fluorescent-tagged glucose bioprobes and their recent structural modifications. *Sensors (Basel) 12*, 5005−5027.

(19) Kim, W. H., Jung, D. W., Kim, J., Im, S. H., Hwang, S. Y., and Williams, D. R. (2012) Small molecules that recapitulate the early steps of urodele amphibian limb regeneration and confer multi-potency. *ACS Chem Biol. 7*, 732−743.

(20) Rosella, G., Zajac, J. D., Kaczmarczyk, S. J., Andrikopoulos, S., and Proietto, J. (1993) Impaired suppression of gluconeogenesis induced by overexpression of a noninsulin-responsive phosphoenol-pyruvate carboxykinase gene. *Mol. Endocrinol. 7*, 1456−1462.

(21) Min, J., Kyung Kim, Y., Cipriani, P. G., Kang, M., Khersonsky, S. M., Walsh, D. P., Lee, J. Y., Niessen, S., Yates, J. R., 3rd, Gunsalus, K., Piano, F., and Chang, Y. T. (2007) Forward chemical genetic approach identifies new role for GAPDH in insulin signaling. *Nat. Chem. Biol. 3*, 55−59.

(22) Elo, B., Villano, C. M., Govorko, D., and White, L. A. (2007) Larval zebrafish as a model for glucose metabolism: expression of phosphoenolpyruvate carboxykinase as a marker for exposure to anti-diabetic compounds. *J. Mol. Endocrinol. 38*, 433−440.

(23) Mitrakou, A. (2011) Kidney: its impact on glucose homeostasis and hormonal regulation. *Diabetes Res. Clin. Pract. 93* (Suppl 1), S66−72.

(24) Hers, H. G. (1990) Mechanisms of blood glucose homeostasis. *J. Inherited Metab. Dis. 13*, 395−410.

(25) Hardie, D. G., and Carling, D. (1997) The AMP-activated protein kinase−fuel gauge of the mammalian cell? *Eur. J. Biochem. 246*, 259−273.

(26) Jensen, P. J., Gunter, L. B., and Carayannopoulos, M. O. (2010) Akt2 modulates glucose availability and downstream apoptotic pathways during development. *J. Biol. Chem. 285*, 17673−17680.

(27) Yang, Y., Shang, W., Zhou, L., Jiang, B., Jin, H., and Chen, M. (2007) Emodin with PPARgamma ligand-binding activity promotes adipocyte differentiation and increases glucose uptake in 3T3-Ll cells. *Biochem. Biophys. Res. Commun. 353*, 225−230.

(28) Tseng, Y. C., Chen, R. D., Lee, J. R., Liu, S. T., Lee, S. J., and Hwang, P. P. (2009) Specific expression and regulation of glucose transporters in zebrafish ionocytes. *Am. J. Physiol.: Regul., Integr. Comp. Physiol. 297*, R275−290.

(29) Agabegi, E., and Steven, S. (2008) *Step-Up to Medicine (Step-Up Series)*, Lippincott Williams & Wilkins, Philadelphia, PA.

(30) Zeng, X. Y., Zhou, X., Xu, J., Chan, S. M., Xue, C. L., Molero, J. C., and Ye, J. M. (2012) Screening for the efficacy on lipid accumulation in 3T3-L1 cells is an effective tool for the identification of new anti-diabetic compounds. *Biochem. Pharmacol. 84*, 830−837.

(31) Madsen, L., Petersen, R. K., Sorensen, M. B., Jorgensen, C., Hallenborg, P., Pridal, L., Fleckner, J., Amri, E. Z., Krieg, P., Furstenberger, G., Berge, R. K., and Kristiansen, K. (2003) Adipocyte differentiation of 3T3-L1 preadipocytes is dependent on lipoxygenase activity during the initial stages of the differentiation process. *Biochem. J. 375*, 539−549.

(32) Chait, A. (1987) Progression of atherosclerosis: the cell biology. *Eur. Heart J. 8* (Suppl E), 15−22.

(33) Zhang, E., Hatada, M., Brewer, J. M., and Lebioda, L. (1994) Catalytic metal ion binding in enolase: the crystal structure of an

enolase-Mn2+-phosphonoacetohydroxamate complex at 2.4-A resolution. *Biochemistry 33*, 6295−6300.
(34) Brewer, J. M., McKinnon, J. S., and Phillips, R. S. (2010) Stopped-flow studies of the reaction of D-tartronate semialdehyde-2-phosphate with human neuronal enolase and yeast enolase 1. *FEBS Lett. 584*, 979−983.
(35) Spring, T. G., and Wold, F. (1971) Studies on two high-affinity enolase inhibitors. Reaction with enolases. *Biochemistry 10*, 4655−4660.
(36) Mansour, H. H., and Tawfik, S. S. (2011) Efficacy of lycopene against fluoride toxicity in rats. *Pharm Biol. 50*, 707−711.
(37) Manneck, T., Keiser, J., and Muller, J. (2012) Mefloquine interferes with glycolysis in schistosomula of Schistosoma mansoni via inhibition of enolase. *Parasitology 139*, 497−505.
(38) Jeffery, C. J. (1999) Moonlighting proteins. *Trends Biochem. Sci. 24*, 8−11.
(39) Miles, L. A., Dahlberg, C. M., Plescia, J., Felez, J., Kato, K., and Plow, E. F. (1991) Role of cell-surface lysines in plasminogen binding to cells: identification of alpha-enolase as a candidate plasminogen receptor. *Biochemistry 30*, 1682−1691.
(40) Liu, K.-J., and Shih, N.-Y. (2007) The role of enolase in tissue invasion and metastasis of pathogens and tumor cells. *J. Cancer Mol. 3*, 45−48.
(41) Walsh, J. L., Keith, T. J., and Knull, H. R. (1989) Glycolytic enzyme interactions with tubulin and microtubules. *Biochim. Biophys. Acta 999*, 64−70.
(42) Li, Z., and Rich, J. N. (2010) Hypoxia and hypoxia inducible factors in cancer stem cell maintenance. *Curr. Top. Microbiol. Immunol. 345*, 21−30.
(43) O'Brien, R. M., Lucas, P. C., Forest, C. D., Magnuson, M. A., and Granner, D. K. (1990) Identification of a sequence in the PEPCK gene that mediates a negative effect of insulin on transcription. *Science 249*, 533−537.
(44) Quinn, P. G., and Yeagley, D. (2005) Insulin regulation of PEPCK gene expression: a model for rapid and reversible modulation. *Curr. Drug Target:s Immune, Endocr. Metab. Disord. 5*, 423−437.
(45) Iori, E., Millioni, R., Puricelli, L., Arrigoni, G., Lenzini, L., Trevisan, R., James, P., Rossi, G. P., Pinna, L. A., and Tessari, P. (2008) Glycolytic enzyme expression and pyruvate kinase activity in cultured fibroblasts from type 1 diabetic patients with and without nephropathy. *Biochim. Biophys. Acta 1782*, 627−633.
(46) Sekiya, M., Osuga, J., Nagashima, S., Ohshiro, T., Igarashi, M., Okazaki, H., Takahashi, M., Tazoe, F., Wada, T., Ohta, K., Takanashi, M., Kumagai, M., Nishi, M., Takase, S., Yahagi, N., Yagyu, H., Ohashi, K., Nagai, R., Kadowaki, T., Furukawa, Y., and Ishibashi, S. (2009) Ablation of neutral cholesterol ester hydrolase 1 accelerates atherosclerosis. *Cell Metab. 10*, 219−228.
(47) Gallagher, E. J., and LeRoith, D. (2011) Diabetes, cancer, and metformin: connections of metabolism and cell proliferation. *Ann. N.Y. Acad. Sci. 1243*, 54−68.
(48) Hynes, M. J., Szewczyk, E., Murray, S. L., Suzuki, Y., Davis, M. A., and Sealy-Lewis, H. M. (2007) Transcriptional control of gluconeogenesis in Aspergillus nidulans. *Genetics 176*, 139−150.
(49) Jurczyk, A., Roy, N., Bajwa, R., Gut, P., Lipson, K., Yang, C., Covassin, L., Racki, W. J., Rossini, A. A., Phillips, N., Stainier, D. Y., Greiner, D. L., Brehm, M. A., Bortell, R., and diIorio, P. (2011) Dynamic glucoregulation and mammalian-like responses to metabolic and developmental disruption in zebrafish. *Gen. Comp. Endrocrinol. 170*, 334−345.
(50) Selderslaghs, I. W., Blust, R., and Witters, H. E. (2012) Feasibility study of the zebrafish assay as an alternative method to screen for developmental toxicity and embryotoxicity using a training set of 27 compounds. *Reprod. Toxicol. 33*, 142−154.
(51) Zhu, S., Lee, J. S., Guo, F., Shin, J., Perez-Atayde, A. R., Kutok, J. L., Rodig, S. J., Neuberg, D. S., Helman, D., Feng, H., Stewart, R. A., Wang, W., George, R. E., Kanki, J. P., and Look, A. T. (2012) Activated ALK collaborates with MYCN in neuroblastoma pathogenesis. *Cancer Cell 21*, 362−373.
(52) Ghosh, A. K., and Jacobs-Lorena, M. (2011) Surface-expressed enolases of Plasmodium and other pathogens. *Mem. Inst. Oswaldo Cruz 106* (Suppl 1), 85−90.